Motor adaptation as a process of re-optimization

Supplementary Information

Jun Izawa, Tushar Rane, Opher Donchin, and Reza Shadmehr

Here we provide details for the simulation results that were presented in the main text. We begin with the optimal control problem with the linear model of dynamics and consider the issue of model uncertainty. We analyze the robustness of the results (over-compensation, speed changes, segmentation) with respect to parameter values. Next, we consider the effect of motor noise. In the final section, we turn our attention to nonlinear models of reach dynamics and examine the robustness of some of the results in a more realistic model of the arm.

1. Optimal control with model noise

In a typical control problem, one attempts to achieve a behavioral goal based on the information that one has regarding the constraints of the task. In optimal control, behavioral goals are represented as costs, and the constraints are represented as a model of the forward dynamics of the task, i.e., a model of how motor commands produce changes in the states of the system. We wanted to allow the controller to have a degree of uncertainty about its forward model and assess how this uncertainty affected movement planning.

In general, we can think of uncertainty as a measure of variance about the mean of a parameter. If the system is linear, then model parameters multiply states of the system to predict future states, and therefore this parameter variability would produce signal-dependent *state* noise. That is, a noise with a standard deviation that grows linearly with the size of the state vector. To solve this kind of optimal control problem, we were guided by the approach taken by Todorov (2005) in solving a related problem, where the dynamics of the system were affected by signal dependent *motor* noise. Our insight was to view model parameter uncertainty as a signal-dependent state noise, that is, a dual to the signal-dependent motor noise.

Suppose that we have a linear system with $\mathbf{x}_t$ as its state vector (position, velocity, etc.) at time t, $\mathbf{u}_t$ as the motor command vector composed of elements $u_t^{(i)}$, corrupted by the noise vector $\boldsymbol{\varphi}_t$, ε as a scalar, Gaussian random variable with zero mean and variance 1, $\varepsilon \sim N(0,1)$, and A and B as matrices that describe dynamics of the system:

$$\mathbf{x}_{t+1} = A\mathbf{x}_t + B\left(\mathbf{u}_t + \boldsymbol{\varphi}_t\right)$$

$$\boldsymbol{\varphi}_t \equiv \begin{bmatrix} c_1 u_t^{(1)} \varepsilon_t^{(1)} & 0 & 0 \\ 0 & c_2 u_t^{(2)} \varepsilon_t^{(2)} & 0 \\ 0 & 0 & \ddots \end{bmatrix}$$

For example, the noise that affects $u_t^{(1)}$ is mean zero with a standard deviation that grows with a slope c_1 as a function of $u_t^{(1)}$. Following Todorov (2005), it is convenient to rewrite this noise as follows:

$$C_1 \equiv \begin{bmatrix} c_1 & 0 & 0 \\ 0 & 0 & 0 \\ 0 & 0 & \ddots \end{bmatrix} \quad C_2 \equiv \begin{bmatrix} 0 & 0 & 0 \\ 0 & c_2 & 0 \\ 0 & 0 & \ddots \end{bmatrix}$$

$$\boldsymbol{\varphi}_t = \sum_i C_i \mathbf{u}_t \varepsilon_t^{(i)}$$

so that the variance of the motor noise grows as a function of the motor input:

$$\text{var}\left[\boldsymbol{\varphi}_t\right] = \sum_i C_i \mathbf{u}_t \, \text{var}\left[\varepsilon_t^{(i)}\right] \mathbf{u}_t^T C_i^T = \sum_i C_i \mathbf{u}_t \mathbf{u}_t^T C_i^T$$

This allows one to rewrite the system dynamics:

$$\mathbf{x}_{t+1} = A\mathbf{x}_t + B\mathbf{u}_t + \sum_{i=1}^{c} \varepsilon_t^{(i)} C_i \mathbf{u}_t$$

If we assume that the controller makes an observation $\mathbf{y}_t$ at time *t*, and has the goal of minimizing a cost:

$$\text{Observation:} \quad \mathbf{y}_t = H\mathbf{x}_t + \boldsymbol{\omega}_t \tag{0.1}$$

$$\text{Cost per step:} \quad \mathbf{x}_t{}^T Q_t \mathbf{x}_t + \mathbf{u}_t{}^T R \mathbf{u}_t \tag{0.2}$$

where $\boldsymbol{\omega}_t \sim N(0, \Omega^{\omega})$, and the matrices Q_t and R are symmetric positive definite matrices, then Todorov's (2005) method provides a closed-form solution to this constrained optimization problem.

In our scenario, we have the additional problem that we are uncertain about the parameter *A*. We express this uncertainty as:

$$\mathbf{x}_{t+1} = (A + \gamma_t V)\mathbf{x}_t + B\mathbf{u}_t + \sum_{i=1}^{c} \varepsilon_t^{(i)} C_i \mathbf{u}_t$$

where γ_t is a Gaussian scalar random variable with mean 0 and standard deviation 1, and *V* is a scaling parameter matrix which scales the variance of the model parameter uncertainty. This effectively produces a system where the dynamics have both a signal dependent motor noise and a signal dependent sensory noise.

In our simulations, we assume that the dynamics were of the following general form:

$$\text{Dynamics:}\quad \mathbf{x}_{t+1} = A\mathbf{x}_t + B\mathbf{u}_t + \boldsymbol{\xi}_t + \sum_{i=1}^{c} \varepsilon_t^{(i)} C_i \mathbf{u}_t + \sum_{i=1}^{k} \gamma_t^{(i)} \overline{C}_i \mathbf{x}_t \tag{0.3}$$

where $\boldsymbol{\xi}_t \sim N(0, \Omega^{\xi})$ is an additive vector of Gaussian noise, $\varepsilon_t^{(i)}$ and $\gamma_t^{(i)}$ are independent scalar normal random variables, and C_i and $\overline{C}_i$ are constant matrices. The initial state $\mathbf{x}_1$ had multivariate normal distribution with mean $\hat{\mathbf{x}}_1$ and covariance Σ_1. The objective of the optimal controller was to find the optimal policy $\mathbf{u}_t$ which minimized the expected cumulative cost $E\left(\sum_{t=1}^{T}(\mathbf{x}_t^T Q_t \mathbf{x}_t + \mathbf{u}_t^T R \mathbf{u}_t)\right)$. We computed the optimal control policy for a pre-calculated Kalman gain K_t as:

$$\begin{aligned}
&\mathbf{u}_t = -L_t \hat{\mathbf{x}}_t \\
&L_t = \left(R + B^T S_{t+1}^x B + \sum_i C_i^T \left(S_{t+1}^x + S_{t+1}^e \right) C_i \right)^{-1} B^T S_{t+1}^x A. \\
&S_t^x = Q_t + A^T S_{t+1}^x \left(A - BL_t \right) + \sum_i \overline{C}_i^T \left(S_{t+1}^x + S_{t+1}^e \right) \overline{C}_i; \quad S_n^x = Q_n \\
&S_t^e = A^T S_{t+1}^x B L_t + \left(A - K_t H \right)^T S_{t+1}^e \left(A - K_t H \right); \quad S_n^e = 0 \\
&s_t = Tr\left(S_{t+1}^x \Omega^{\xi} + S_{t+1}^e \left(\Omega^{\xi} + \Omega^{\eta} + K_t \Omega^{\omega} K_t^T \right) \right) + s_{t+1}; \quad s_n = 0.
\end{aligned} \tag{0.4}$$

The matrix L_t is the time-varying feedback gain, and S_t^e, S_t^x are the parameters required to calculate the optimal cost-to-go function at any time step t. *Tr* is the trace operator. The state estimate is updated by using a modified Kalman filter which takes into account the multiplicative noise. For a given feedback gain matrix L_t, the corresponding optimal Kalman filter is calculated in a forward pass through time:

$$\begin{aligned}
&\hat{\mathbf{x}}_{t+1} = \left(A - BL_t \right) \hat{\mathbf{x}}_t + K_t \left(\mathbf{y}_t - H \hat{\mathbf{x}}_t \right) + \eta_t \\
&K_t = A \Sigma_t^e H^T \left(H \Sigma_t^e H^T + \Omega^{\omega} \right)^{-1} \\
&\Sigma_{t+1}^e = \Omega^{\xi} + \Omega^{\eta} + \sum_i \left(\overline{C}_i \left(\Sigma_t^e + \Sigma_t^{\hat{x}} + 2\Sigma_t^{\hat{x}e} \right) \overline{C}_i^T + C_i L_t \Sigma_t^{\hat{\mathbf{x}}} L_t^T C_i^T \right) + \left(A - K_t H \right) \Sigma_t^e A^T \\
&\Sigma_1^e = \Sigma_1 \\
&\Sigma_{t+1}^{\hat{x}} = \left(A - BL_t \right) \Sigma_t^{\hat{x}} \left(A - BL_t \right)^T + K_t H \Sigma_t^e A^T + \left(A - BL_t \right) \Sigma_t^{\hat{x}e} H^T K_t^T + K_t H \Sigma_t^{\hat{x}e} \left(A - BL_t \right)^T + \Omega^{\eta} \\
&\Sigma_1^{\hat{x}} = \hat{\mathbf{x}}_1 \hat{\mathbf{x}}_1^T \\
&\Sigma_{t+1}^{\hat{x}e} = \left(A - BL_t \right) \Sigma_t^{\hat{x}e} \left(A - K_t H \right)^T - \Omega^{\eta}
\end{aligned} \tag{0.5}$$

The matrices, K_t, $\Sigma_t^e = E[\mathbf{e}_t \mathbf{e}_t^T]$, $\Sigma_t^{\hat{x}} = E[\hat{\mathbf{x}}_t \hat{\mathbf{x}}_t^T]$ and $\Sigma_t^{\hat{x}e} = E[\hat{\mathbf{x}}_t \mathbf{e}_t^T]$ are the optimal Kalman gain and the covariance matrices for the random variables $\mathbf{e}_t = \mathbf{x}_t - \hat{\mathbf{x}}_t$ and $\hat{\mathbf{x}}_t$.

The details of the derivation are provided at the end of this document.

2. Dynamics of the linear system model of reach control

Much of the data in the main manuscript was based on a model of control for a point mass in a force field. This section provides the details of that model. The inertia in Cartesian coordinates was $M = \begin{bmatrix} 4.0 & 0 \\ 0 & 1.5 \end{bmatrix}$ (kg). The state was defined as $\mathbf{x}(t) = [\, p_x(t),\, \dot{p}_x(t),\, p_y(t),\, \dot{p}_y(t),\, f_x(t),\, f_y(t), T_x, T_y \,]$, where $p_x(t)$, $p_y(t)$ and $f_x(t),\, f_y(t)$ and T_x, T_y are the hand position, forces produced by the arm, and target position along the x and y axes respectively. We modeled the relationship between forces $f_x(t),\, f_y(t)$ and the motor commands $u_x(t), u_y(t)$ as a first order linear system with a 120ms time constant.

We tested the optimal control policies predicted by the model in a viscous curl force field. This kind of field is velocity dependent and the forces produced on the hand are given by the relation $\mathbf{f} = D\mathbf{v}$, where $D = \begin{bmatrix} d_{11} & d_{12} \\ d_{21} & d_{22} \end{bmatrix}$ and $\mathbf{v}$ is a hand velocity vector. We discretized the system dynamics with a time step of $\Delta t = 10ms$. The evolution of different components of the state for this discretized system is as follws:

$$
\begin{aligned}
\begin{bmatrix} p_x(t+\Delta t) \\ p_y(t+\Delta t) \end{bmatrix} &= \begin{bmatrix} p_x(t) \\ p_y(t) \end{bmatrix} + \Delta t \begin{bmatrix} \dot{p}_x(t) \\ \dot{p}_y(t) \end{bmatrix} \\
\begin{bmatrix} \dot{p}_x(t+\Delta t) \\ \dot{p}_y(t+\Delta t) \end{bmatrix} &= \begin{bmatrix} \dot{p}_x(t) \\ \dot{p}_y(t) \end{bmatrix} + \Delta t \begin{pmatrix} \frac{d_{11}}{m_1} & \frac{d_{12}}{m_2} \\ \frac{d_{21}}{m_1} & \frac{d_{22}}{m_2} \end{pmatrix} \begin{bmatrix} \dot{p}_x(t) \\ \dot{p}_y(t) \end{bmatrix} + \Delta t \begin{bmatrix} \frac{f_x(t)}{m_1} \\ \frac{f_y(t)}{m_2} \end{bmatrix} + \Delta t \cdot \gamma \cdot \begin{pmatrix} \frac{d_{11}}{m_1} & \frac{d_{12}}{m_2} \\ \frac{d_{21}}{m_1} & \frac{d_{22}}{m_2} \end{pmatrix} \qquad (0.6) \\
\begin{bmatrix} f_x(t+\Delta t) \\ f_y(t+\Delta t) \end{bmatrix} &= \begin{bmatrix} 1-\frac{\Delta t}{\tau} & 0 \\ 0 & 1-\frac{\Delta t}{\tau} \end{bmatrix} \begin{bmatrix} f_x(t) \\ f_y(t) \end{bmatrix} + \frac{\Delta t}{\tau} \begin{bmatrix} u_x(t) \\ u_y(t) \end{bmatrix}
\end{aligned}
$$

where γ is a mean zero variance σ^2 Gaussian noise. The discretized system dynamics can be transformed into the form of Eqn. (0.3) using the matrices:

$$A = \begin{bmatrix} A_d & 0 & 0 \\ 0 & 1 & 0 \\ 0 & 0 & 1 \end{bmatrix} \qquad A_d = \begin{bmatrix} 1 & \Delta t & 0 & 0 & 0 & 0 \\ 0 & 1+\Delta t\frac{d_{11}}{m_1} & 0 & \Delta t\frac{d_{12}}{m_1} & \Delta t\frac{1}{m_1} & 0 \\ 0 & 0 & 1 & \Delta t & 0 & 0 \\ 0 & \Delta t\frac{d_{21}}{m_2} & 0 & 1+\Delta t\frac{d_{22}}{m_2} & 0 & \Delta t\frac{1}{m_2} \\ 0 & 0 & 0 & 0 & 1-\frac{\Delta t}{\tau} & 0 \\ 0 & 0 & 0 & 0 & 0 & 1-\frac{\Delta t}{\tau} \end{bmatrix}$$

$$B = \begin{bmatrix} 0_{4X2} \\ \frac{\Delta t}{\tau} \quad 0 \\ 0 \quad \frac{\Delta t}{\tau} \\ 0_{2X2} \end{bmatrix} \qquad C_1 = \begin{bmatrix} C_{d1} & 0 & 0 \\ 0 & 1 & 0 \\ 0 & 0 & 1 \end{bmatrix} \; C_{d1} = \begin{bmatrix} 0 & 0 & 0 & 0 & 0 & 0 \\ 0 & \sigma\sqrt{\Delta t}\frac{d_{11}}{m_1} & 0 & \sigma\sqrt{\Delta t}\frac{d_{12}}{m_1} & 0 & 0 \\ 0 & 0 & 0 & 0 & 0 & 0 \\ 0 & \sigma\sqrt{\Delta t}\frac{d_{21}}{m_2} & 0 & \sigma\sqrt{\Delta t}\frac{d_{22}}{m_2} & 0 & 0 \\ 0 & 0 & 0 & 0 & 0 & 0 \\ 0 & 0 & 0 & 0 & 0 & 0 \end{bmatrix} \qquad (0.7)$$

$$\bar{C} = \left[0_{8X2}\right]$$

The sensory feedback matrix was formulated so that the controller was able to observe hand positions, velocities and the target positions over the course of the movement. Hence,

$$H = \begin{bmatrix} 1 & 0 & 0 & 0 & 0 & 0 & 0 & 0 \\ 0 & 0 & 1 & 0 & 0 & 0 & 0 & 0 \\ 0 & 1 & 0 & 0 & 0 & 0 & 0 & 0 \\ 0 & 0 & 0 & 1 & 0 & 0 & 0 & 0 \\ 0 & 0 & 0 & 0 & 0 & 0 & 1 & 0 \\ 0 & 0 & 0 & 0 & 0 & 0 & 0 & 1 \end{bmatrix}.$$

The control (or motor) cost penalty matrix *R* was set to a constant value throughout the course of the movement. The parameter w_r determines the weight of the control cost. We set $R = w_r I_{2X2}$ for $0 \le t < T + T_H$ where *T* is the maximum movement completion time and T_H is the time for which the arm was supposed to hold position at the target after movement completion.

The 'state cost' penalty matrix was formulated so that the state cost was zero before the movement completion time *T* and was increased in a step to a high value for the time period from T to T_H . This formulation provided the controller with the maximum flexibility to search for the optimal policy since the controller was penalized only for not being at the target after the movement completion time *T* without

imposing any constraints on the trajectory followed by the controller to reach the target.

$Q = [0_{8X8}]$ for $0 \le t < T$ and

$$Q = \begin{bmatrix} w_p & 0 & 0 & 0 & 0 & 0 & -w_p & 0 \\ 0 & w_v & 0 & 0 & 0 & 0 & 0 & 0 \\ 0 & 0 & w_p & 0 & 0 & 0 & 0 & -w_p \\ 0 & 0 & 0 & w_v & 0 & 0 & 0 & 0 \\ 0 & 0 & 0 & 0 & w_f & 0 & 0 & 0 \\ 0 & 0 & 0 & 0 & 0 & w_f & 0 & 0 \\ -w_p & 0 & 0 & 0 & 0 & 0 & w_p & 0 \\ 0 & 0 & -w_p & 0 & 0 & 0 & 0 & w_p \end{bmatrix} \text{ for } T \le t < T + T_H$$

.

For simplicity, the variance of the additive Gaussian noises was set to zero.

$$\Omega^{\xi} = \mathbf{0}$$
$$\Omega^{\omega} = \mathbf{0}.$$

The cost parameters and the time constraints used for the simulations in the manuscript were:

$w_r = 10^{-8}, w_v = 0.01, w_f = 0, w_p = 5, T = \frac{0.45}{\Delta t}, T_H = \frac{0.05}{\Delta t}$. Sensitivity of the simulations to these parameters are discussed below.

3. Effect of bias of the forward model on the optimal control policy: sensitivity analysis

This section describes how we simulated the effects of incomplete adaptation of the internal model on the average behavior of the controller for the point mass system. This section also considers the robustness of the results by varying components of the cost function.

The estimate of the force field parameter available to the controller through the internal model was $\hat{D} = \alpha \bar{D}$. Scaling parameter α denotes accuracy of internal model corresponding to force field. The simulation results shown in Fig. S1 correspond to a clockwise viscous curl force field where $\bar{D} = \begin{bmatrix} 0 & 13 \\ -13 & 0 \end{bmatrix}$. The simulations were done for three different levels of accuracy of the internal model $\alpha = 1,\ 0.8$ and 0.6. We also explored the effects of various levels of the position cost parameter w_p on the simulation results. We found that a completely adapted internal model $\alpha = 1$ led to over-compensation. However, as the adaptation level decreased $(\alpha = 0.8 \text{ and } 0.6)$, the over-compensation at the early part of the movement became smaller as the under-compensation near the

target increased.

As the position cost parameter w_p decreased, the trajectory did not complete the reaching to target position. However, the over-compensation was a characteristics of all tested values of w_p.

4. Effect of uncertainty of the internal model: sensitivity analysis

In this simulation, the internal model was defined as $\hat{D} = \alpha\bar{D} + \gamma_t\bar{D}$, where γ_t is a zero mean Gaussian random variable with variance σ^2. Figure S2A shows how the variance of this noise and position cost w_p interact. In the simulations, we had $\alpha = 0.8$. The results plotted by blue, red and green lines denote different amounts of uncertainty σ=0.1, σ=0.2 and σ=0.3 respectively. When position costs were small ($w_p = 10^{-4}, 10^{-3}, 10^{-2}, 10^{-1}$), the mass did not reach the target and peak velocity was small for all σ. When this cost was larger ($w_p = 10^{0}, 10^{1}, 10^{2}, 10^{3}$), the mass reached the target and there were clear differences in peak velocity between σ=0, 0.2 and 0.3 such that higher noise caused higher peak velocity. In all cases, the peak velocity was higher with higher noise.

Figure S2B shows the effect of noise for different level of w_r (control cost). When this weight was too large ($w_r = 10^{-6}, 10^{-5}$), the mass did not reach the target. When this weight was smaller ($w_r = 10^{-12}, 10^{-11}, 10^{-10}, 10^{-9}, 10^{-8}, 10^{-7}$), the mass reached the target and there were clear differences in peak velocity between σ=0.1, 0.2 and 0.3 so that higher noise caused higher peak velocity. In general, the prediction of increased peak speed with increased uncertainty was a robust result of the simulations.

5. Effects of model uncertainty in the via point task: sensitivity analysis

The task was to arrive at the target before certain maximum time T and stay there for a hold time of T_H while passing through the via-point (a location along a straight line between the starting position and the target) at a specific via-point time T_V. These simulations were performed for an unbiased viscous curl force field, i.e. the components of the matrix *D* are all zero. Hence, any differences in the optimal control policy are purely due to different levels of uncertainties without being confounded with incomplete learning of the force field parameter *D*. The state for the via-point task was modified to include the location of the via-point. All other components of the state were the same.

$$\mathbf{x}(t) = [\, p_x(t),\, \dot{p}_x(t),\, p_y(t),\, \dot{p}_y(t),\, f_x(t),\, f_y(t), TV_x, TV_y, T_x, T_y\,]$$

where TV_x, TV_y are x and y co-ordinates of the via point location. The system dynamics matrices were modified to incorporate the via-point location in the state vector. We made small modifications to the matrices so that the via-point location remained constant over the course of the movement as shown below. All other components of these matrices remain the same as in the simple reaching task.

$$A = \begin{bmatrix} A_d & 0 \\ 0 & I_{4X4} \end{bmatrix} \qquad B = \begin{bmatrix} 0_{4X2} \\ \frac{\Delta t}{\tau} \quad 0 \\ 0 \quad \frac{\Delta t}{\tau} \\ 0_{4X2} \end{bmatrix} \qquad C_1 = \begin{bmatrix} C_{d1} & 0 \\ 0 & I_{4X4} \end{bmatrix} \qquad \bar{C} = \begin{bmatrix} 0_{10X2} \end{bmatrix}$$

where A_d and C_{d1} were the same as Eqn 0.7.

The sensory feedback matrix *H* was changed so that the observation $\mathbf{y}$ included the via-point location.

$$H = \begin{bmatrix} 1 & 0 & 0 & 0 & 0 & 0 & 0 & 0 & 0 & 0 \\ 0 & 0 & 1 & 0 & 0 & 0 & 0 & 0 & 0 & 0 \\ 0 & 1 & 0 & 0 & 0 & 0 & 0 & 0 & 0 & 0 \\ 0 & 0 & 0 & 1 & 0 & 0 & 0 & 0 & 0 & 0 \\ 0 & 0 & 0 & 0 & 0 & 0 & 1 & 0 & 0 & 0 \\ 0 & 0 & 0 & 0 & 0 & 0 & 0 & 1 & 0 & 0 \\ 0 & 0 & 0 & 0 & 0 & 0 & 0 & 0 & 1 & 0 \\ 0 & 0 & 0 & 0 & 0 & 0 & 0 & 0 & 0 & 1 \end{bmatrix}.$$

The control cost penalty matrix *R* was the same as in previous section. However, we had to modify the 'state cost' penalty matrix to penalize the controller for not being at the via-point at the via-point time. The variance of the additive Gaussian noises $\left(\Omega^{\xi}, \Omega^{\omega}\right)$ was set to zero similar to the simulations for the reaching task.

The cost parameters and the time constraints used for the via-point simulations in the manuscript were $w_r = 10^{-8},\, w_v = 0.01,\, w_p = 3,\, w_{pv} = 1,\, T = \frac{1.0}{\Delta t},\, T_v = \frac{0.4}{\Delta t},\, T_H = \frac{0.2}{\Delta t}$. To account for the unbiased variable force field, we assumed an internal model which had the model of force field with parameters, $\hat{D} = \gamma_t \bar{D}$, where $\bar{D} = \begin{bmatrix} 0 & 13 \\ -13 & 0 \end{bmatrix}$, γ_t is a Gaussian random variable with mean 0 and variance σ. We

tested σ =0, 0.2, or 0.3.

Figure S3A shows the effect of noise for different values of w_p. The hand path was a straight line for all amplitudes of noise and all costs in all simulations of the via-point task (data not shown). However, with increased uncertainty (noise variance), the speed decreased at the time when hand passed the via-point. This characteristic was consistent for all w_p. As shown in Fig. S3B, the characteristics of the decreasing speed at the via point changed drastically by the change of weight of via point w_{pv}. When w_{pv} was very small ($w_{pv} = 10^{-3}, 10^{-2}, 10^{-1}$), there was effectively no strong cost associated with going through the via-point, and the speed profile did not show segmentation. However, as the constraint for going through the via-point increased in importance, the speed profile became bimodal. Fig. S3C shows trajectories for different control costs w_r. When w_r was large ($w_r = 10^{-6}, 10^{-5}, 10^{-4}$), the mass did not reach the target, indicating that optimal controller focused more on minimizing motor cost than the cost for reach. Thus, the change of speed at via point was not significant for these conditions. Instead, when w_r was small ($w_r = 10^{-11}, 10^{-10}, 10^{-9}, 10^{-8}, 10^{-7}$), there was a significant change of speed at the via-point, producing segmentation. We concluded that in the via point task, increased uncertainty consistently encouraged segmentation.

6. Effect of motor noise

Noise in the motor commands is an important component of the computational models of the motor system (Harris and Wolpert, 1998; Todorov and Jordan, 2002). We excluded motor command dependent noise in the simulations shown in the manuscript to highlight the effects of model parameter uncertainty on the optimal control policy. In this section we address the issue of the effect of different levels of motor command dependent noise on the model predictions. The parameter c lets us control the variance of the signal dependent motor noise in the system.

$$C = \begin{bmatrix} 0 & 0 & 0 & 0 & \sqrt{\Delta t}\, c & 0 & 0 & 0 \\ 0 & 0 & 0 & 0 & 0 & \sqrt{\Delta t}\, c & 0 & 0 \end{bmatrix}^T$$ for the point-to-point reach task

and

$$C = \begin{bmatrix} 0 & 0 & 0 & 0 & \sqrt{\Delta t}\, c & 0 & 0 & 0 & 0 & 0 \\ 0 & 0 & 0 & 0 & 0 & \sqrt{\Delta t}\, c & 0 & 0 & 0 & 0 \end{bmatrix}^T$$ for the via-point task.

Figure S4A shows the simulation results for different amounts of motor command noise (i.e. c). All other parameters were kept constant at the values used for the simulations shown in the manuscript. All simulations were repeated for three different levels of model parameter uncertainty (σ =0, 0.2 and 0.3, corresponding to the blue, red, and green lines in this figure). The mass failed to reach the end point and the effects of model parameter uncertainty on the speed profile were unclear for high values of motor noise ($c > 0.08$). On the other hand, the characteristics of trajectory with respect to the model parameter uncertainty were consistent with the results shown in the manuscript for low values of motor noise ($c < 0.08$): an increase in model parameter uncertainty made over compensation decrease and peak velocity increase. Large amounts of motor noise caused slowness of movement, indicating the effect of motor noise is similar to effect of motor cost.

Figure S4B shows the results for different levels of motor noise in the via-point task. The results show a segmented movement as long as the motor noise is low to moderate ($c < 0.08$). With very large motor noise, the segmentation disappears. However, in all cases the increase uncertainty causes the speed profiles to become skewed with a sharper rise as the movement initiates.

In the representative paper concerning motor noise (Todorov and Jordan, 2002), the scaling parameter was set as 0.04. In experiments on arm muscles, the scaling parameter of signal dependent noise is thought to be around 0.05 (Hamilton et al., 2004) . Our simulations also found clear effects of model uncertainty when motor noise amplitude was around 0.06 or smaller.

7. Solving the optimal control problem with model uncertainty

In this section, we drive the solution to the optimal control problem with model uncertainty. Consider a linear dynamical system with state $\mathbf{x}_t \in R^m$, control signal $\mathbf{u}_t \in R^p$, feedback $\mathbf{y}_t \in R^q$, in discrete time *t*:

Dynamics $$\mathbf{x}_{t+1} = A\mathbf{x}_t + B\mathbf{u}_t + \boldsymbol{\xi}_t + \sum_{i=1}^{c} \gamma_t^i C_i \mathbf{x}_t + \sum_{i=1}^{c} \varepsilon_t^i \bar{C}_i \mathbf{u}_t \qquad (0.8)$$

Feedback $$\mathbf{y}_t = H\mathbf{x}_t + \boldsymbol{\omega}_t \qquad (0.9)$$

Cost per step $$\mathbf{x}_t^T Q_t \mathbf{x}_t + \mathbf{u}_t^T R \mathbf{u}_t \qquad (0.10)$$

The state estimate of the dynamic system available to the controller is assumed to be updated according to a linear recursive filter for analytical tractability.

$$\hat{\mathbf{x}}_{t+1} = A\hat{\mathbf{x}}_t + B\mathbf{u}_t + K_t\left(y_t - H\hat{\mathbf{x}}_t\right) + \eta_t$$

We define the estimation error as $\mathbf{e}_t = \mathbf{x}_t - \hat{\mathbf{x}}_t$. We can show through induction that the optimal

cost-to-go function or the cost expected to accumulate under the optimal control law after a time step *t* has the quadratic form.

$$v_t(\mathbf{x}_t, \hat{\mathbf{x}}_t) = \mathbf{x}_t^T S_t^x \mathbf{x}_t + (\mathbf{x}_t - \hat{\mathbf{x}}_t)^T S_t^e (\mathbf{x}_t - \hat{\mathbf{x}}_t) + s_t = \mathbf{x}_t^T S_t^x \mathbf{x}_t + \mathbf{e}_t^T S_t^e \mathbf{e}_t + s_t \tag{0.11}$$

At the final time $t = n$, the optimal cost-to-go function is simply the final state cost $\mathbf{x}_n^T Q_n \mathbf{x}_n$, and so v_n is in the assumed form with $S_n^x = Q_n$, $S_n^e = 0$, s_n.

Consider the optimal control policy denoted by $\mathbf{u}_t = \pi(\hat{\mathbf{x}}_t)$. Let $v_{t+1}^{\pi}(\mathbf{x}_t, \hat{\mathbf{x}}_t)$ be the cost-to-go function corresponding to the optimal control law. Since this control law is optimal for all time points *t*+1,…,*n*, we have $v_{t+1}^{\pi} = v_{t+1}$, so that the cost-to-go function v_t^{π} satisfies the Bellman equation:

$$v_t^{\pi}(\mathbf{x}_t, \hat{\mathbf{x}}_t) = \mathbf{x}_t^T Q_t \mathbf{x}_t + \pi(\hat{\mathbf{x}}_t)^T R \pi(\hat{\mathbf{x}}_t) + E[v_{t+1}(\mathbf{x}_{t+1,} \hat{\mathbf{x}}_{t+1}) \mid \mathbf{x}_t, \mathbf{x}_{t,} \pi] \tag{0.12}$$

Now, the stochastic dynamics of the variables of interest can be written as

$$\mathbf{x}_{t+1} = A\mathbf{x}_t + B\mathbf{u}_t + \boldsymbol{\xi}_t + \sum_{i=1}^{c} \gamma_t^i C_i \mathbf{x}_t + \sum_{i=1}^{c} \varepsilon_t^i \bar{C}_i \mathbf{u}_t \tag{0.13}$$

$$\mathbf{e}_{t+1} = (A - K_t H)\mathbf{e}_t + \boldsymbol{\xi}_t - K_t \boldsymbol{\omega}_t - \eta_t + \sum_i \left(\gamma_t^i C_i \mathbf{x}_t + \varepsilon_t^i \bar{C}_i \mathbf{u}_t \right). \tag{0.14}$$

Then the conditional means and co variances of these random variables of interest are

$$\begin{aligned}
\mathrm{E}[\mathbf{x}_{t+1} \mid \mathbf{x}_t, \hat{\mathbf{x}}_t, \pi] &= A\mathbf{x}_t + B\pi(\hat{\mathbf{x}}_t) \\
\mathrm{E}[\mathbf{e}_{t+1} \mid \mathbf{x}_t, \hat{\mathbf{x}}_t, \pi] &= (A - K_t H)\mathbf{e}_t \\
\mathrm{Cov}[\mathbf{x}_{t+1} \mid \mathbf{x}_t, \hat{\mathbf{x}}_t, \pi] &= \Omega^{\xi} + \sum_i \left(C_i \mathbf{x}_t \mathbf{x}_t^T C_i^T + \bar{C}_i \pi(\hat{\mathbf{x}}_t) \pi(\hat{\mathbf{x}}_t)^T \bar{C}_i^T \right) \\
\mathrm{Cov}[\mathbf{e}_{t+1} \mid \mathbf{x}_t, \hat{\mathbf{x}}_t, \pi] &= \Omega^{\xi} + \sum_i \left(C_i \mathbf{x}_t \mathbf{x}_t^T C_i^T + \bar{C}_i \pi(\hat{\mathbf{x}}_t) \pi(\hat{\mathbf{x}}_t)^T \bar{C}_i^T \right) + \Omega^{\eta} + K_t \Omega^{\omega} K_t^T
\end{aligned} \tag{0.15}$$

Using the expected values and the covariances we just found and the relations from Eqn 0.11 and 0.12, we get an expression for the cost-to-go function

$$\begin{aligned}
v_t^{\pi}(\mathbf{x}_t, \hat{\mathbf{x}}_t) = \mathbf{x}_t^T \left(Q_t + A^T S_{t+1}^x A + \sum_i C_i^T (S_{t+1}^x + S_{t+1}^e) C_i \right) \mathbf{x}_t + s_{t+1} + \mathbf{e}_t^T \left(A - K_t H \right)^T S_{t+1}^e \left(A - K_t H \right) \mathbf{e}_t \\
+ Tr(M_t) + \pi\left(\hat{\mathbf{x}}_t\right)^T \left(R + B^T S_{t+1}^x B + \sum_i \bar{C}_i^T (S_{t+1}^x + S_{t+1}^e) \bar{C}_i \right) \pi\left(\hat{\mathbf{x}}_t\right) + 2\pi\left(\hat{\mathbf{x}}_t\right)^T B^T S_{t+1}^x A \mathbf{x}_t
\end{aligned} \tag{0.16}$$

Writing the expression in a compact form, we have

$$
\begin{aligned}
v_t^{\pi}(\mathbf{x}_t, \hat{\mathbf{x}}_t) = \mathbf{x}_t^T \left(Q_t + A^T S_{t+1}^x A + C_t\right)\mathbf{x}_t + \mathbf{e}_t^T \left(A - K_t H\right)^T S_{t+1}^e \left(A - K_t H\right)\mathbf{e}_t \\
+ s_{t+1} + Tr\left(M_t\right) + \pi\left(\hat{\mathbf{x}}_t\right)^T \left(R + B^T S_{t+1}^x B + \bar{C}_t\right)\pi\left(\hat{\mathbf{x}}_t\right) \\
+ 2\pi\left(\hat{\mathbf{x}}_t\right)^T B^T S_{t+1}^x A\mathbf{x}_t
\end{aligned}
\tag{0.17}
$$

Where

$$
\begin{aligned}
C_t &= \sum_i C_i^T (S_{t+1}^x + S_{t+1}^e) C_i \\
\bar{C}_t &= \sum_i \bar{C}_i^T (S_{t+1}^x + S_{t+1}^e) \bar{C}_i \\
M_t &= S_{t+1}^x \Omega^{\xi} + S_{t+1}^e \left(\Omega^{\xi} + \Omega^{\eta} + K_t \Omega^{\omega} K_t^T\right)
\end{aligned}
\tag{0.18}
$$

The cost-to-go function, however, is a function of the true state $\mathbf{x}_t$, which is not available to the controller. The only thing available to the controller is the state estimate $\hat{\mathbf{x}}_t$. So, we take the expected value of the cost-to-go function over the true state and minimize it with respect to the control policy π.

Since $E[\mathbf{x}_t \mid \hat{\mathbf{x}}_t] = \hat{\mathbf{x}}_t$, we have

$$
E[v_t^{\pi}(\mathbf{x}_t, \hat{\mathbf{x}}_t) \mid \hat{\mathbf{x}}_t] = const + \pi(\hat{\mathbf{x}}_t)^T (R + B^T S_{t+1}^x B + \bar{C}_t)\pi(\hat{\mathbf{x}}_t) + 2\pi(\hat{\mathbf{x}}_t)^T B^T S_{t+1}^x A\mathbf{x}_t, \tag{0.19}
$$

Thus optimal control law at time point *t* is

$$
\mathbf{u}_t = \pi(\hat{\mathbf{x}}_t) = -L_t \hat{\mathbf{x}}_t; \quad L_t = (R + B^T S_{t+1}^x B + \bar{C}_t)^{-1} B^T S_{t+1}^x A.
\tag{0.20}
$$

Substituting $\mathbf{u}_t - L_t \hat{\mathbf{x}}_t$ in Eqn 0.16

$$
\begin{aligned}
v^{\pi}(\mathbf{x}_t, \hat{\mathbf{x}}_t) = \mathbf{x}_t^T \left(Q_t + A^T S_{t+1}^x \left(A - BL_t\right) + C_t\right)\mathbf{x}_t + Tr\left(M_t\right) + s_{t+1} \\
+ \mathbf{e}_t^T \left(A^T S_{t+1}^x BL_t + \left(A - K_t H\right)^T S_{t+1}^e \left(A - K_t H\right)\right)\mathbf{e}_t
\end{aligned}
\tag{0.21}
$$

Comparing this equation with Eqn 0.11, we can summarize the optimal control law with the following equations:

$$
\begin{aligned}
&\mathbf{u}_t = -L_t \hat{\mathbf{x}}_t \\
&L_t = \left(R + B^T S_{t+1}^x B + \bar{C}_t\right)^{-1} B^T S_{t+1}^x A. \\
&S_t^x = Q_t + A^T S_{t+1}^x \left(A - BL_t\right) + C_t; \quad S_n^x = Q_n \\
&S_t^e = A^T S_{t+1}^x BL_t + \left(A - K_t H\right)^T S_{t+1}^e \left(A - K_t H\right); \quad S_n^e = 0 \\
&s_t = Tr\left(M_t\right) + s_{t+1}; \quad s_n = 0.
\end{aligned}
\tag{0.22}
$$

Thus, we showed that the cost-to-go function remains in the assumed quadratic form shown in Eqn 0.11 for any time step t given that it is true for the time step t+1, completing the induction proof.

The next step is to calculate the optimal Kalman gains for the control policy we just calculated. According to the assumption in the previous section of the Kalman gains not being functions of $\mathbf{x}_t$ and $\hat{\mathbf{x}}_t$, we need to minimize the unconditional expectation of the cost-to-go function v_{t+1} with respect to K_t to calculate the optimal Kalman gains.

The terms in $E[v_{t+1}(\mathbf{x}_{t+1}, \hat{\mathbf{x}}_{t+1}) \mid \mathbf{x}_t, \hat{\mathbf{x}}_t, L_t]$ that depend on K_t are

$$e_t^T \left(A - K_t H\right)^T S_{t+1}^e \left(A - K_t H\right) e_t + Tr\left(S_{t+1}^e K_t \Omega^\omega K_t^T\right) \tag{0.23}$$

Defining the unconditional covariances $\Sigma_t^e = E[\mathbf{e}_t \mathbf{e}_t^T]$, $\Sigma_t^{\mathbf{x}} = E[\mathbf{x}_t \mathbf{x}_t^T]$ and $\Sigma_t^{\mathbf{xe}} = E[\mathbf{x}_t \mathbf{e}_t^T]$, the unconditional expectation of the K_t-dependent expression above becomes

$$a(K_t) = Tr\left(\left(\left(A - K_t H\right)\Sigma_t^e \left(A - K_t H\right)^T + K_t \Omega^\omega K_t^T\right) S_{t+1}^e\right) \tag{0.24}$$

Optimal K_t must satisfy $\dfrac{\partial a(K_t)}{\partial K_t} = 0$.

$$\frac{\partial a\left(K_t\right)}{\partial K_t} = 2S_{t+1}^e \left(K_t \left(H \Sigma_t^e H^T + \Omega^\omega\right) - A \Sigma_t^e H^T\right) \tag{0.25}$$

Setting the derivative to zero and solving for K_t.

$$K_t = A\Sigma_t^e H^T (H\Sigma_t^e H^T + \Omega^\omega)^{-1} \tag{0.26}$$

We found an expression to calculate the optimal Kalman gains. But, we still need to find the unconditional covariances $\Sigma_t^e, \Sigma_t^{\hat{x}}$ and $\Sigma_t^{\hat{x}e}$. Since the variables $\mathbf{x}, \hat{\mathbf{x}}$ and $\mathbf{e}$ are deterministically related, we can calculate the covariance of the third variable given that we know the covariance for two variables. Given the covariance of $\hat{\mathbf{x}}$ and $\mathbf{e}$, the covariance of $\mathbf{x}$ is given by

$$\Sigma_{t+1}^{\mathbf{x}} = E\left[\left(\mathbf{e} + \hat{\mathbf{x}}\right)\left(\mathbf{e} + \hat{\mathbf{x}}\right)^T\right] = \Sigma_t^{\mathbf{e}} + \Sigma_t^{\hat{\mathbf{x}}} + \Sigma_t^{\hat{\mathbf{x}}\mathbf{e}} + \Sigma_t^{\hat{\mathbf{x}}\mathbf{e}T}$$

Now, using the expressions for $\hat{\mathbf{x}}_{t+1}$ and $\mathbf{e}_{t+1}$, we can calculate the expressions for the unconditional covariances shown below

$$\begin{aligned}\Sigma_{t+1}^e &= (A - K_t H)\Sigma_t^{\mathbf{e}}(A - K_t H)^T + \Omega^\xi + \Omega^\eta + K_t \Omega^\omega K_t^T \\ &\quad + \sum_i \left(C_i \left(\Sigma_t^{\mathbf{e}} + \Sigma_t^{\hat{\mathbf{x}}} + \Sigma_t^{\hat{\mathbf{x}}\mathbf{e}} + \Sigma_t^{\hat{\mathbf{x}}\mathbf{e}T}\right) C_i^T + \bar{C}_i L_t \Sigma_t^{\hat{\mathbf{x}}} L_t^T \bar{C}_i^T\right)\end{aligned}$$

$$\begin{aligned}\Sigma_{t+1}^{\hat{\mathbf{x}}} &= (A - BL_t)\Sigma_t^{\hat{\mathbf{x}}}(A - BL_t)^T + K_t \left(H \Sigma_t^{\mathbf{e}} H^T + \Omega^\omega\right) K_t^T \\ &\quad + (A - BL_t)\Sigma_t^{\hat{\mathbf{x}}\mathbf{e}} H^T K_t^T + K_t H \Sigma_t^{\hat{\mathbf{x}}\mathbf{e}} (A - BL_t)^T + \Omega^\eta\end{aligned}$$

$$\Sigma_{t+1}^{\hat{\mathbf{x}}e} = (A - BL_t)\Sigma_t^{\hat{\mathbf{x}}e}(A - K_tH)^T + K_tH\Sigma_t^{\mathbf{e}}(A - K_tH)^T - K_t\Omega^{\omega}K_t^T - \Omega^{\eta} \quad (0.27)$$

Substituting the expression for K_t from Eqn 0.26 in the above expressions for covariances, we can simplify them further to get the following system of equations which lets us calculate the optimal Kalman gains in a forward pass through time

$$\begin{aligned}
\hat{\mathbf{x}}_{t+1} &= (A - BL_t)\hat{\mathbf{x}}_t + K_t(\mathbf{y}_t - H\hat{\mathbf{x}}_t) + \eta_t \\
K_t &= A\Sigma_t^e H^T(H\Sigma_t^e H^T + \Omega^{\omega}) \\
\Sigma_{t+1}^e &= \Omega^{\xi} + \Omega^{\eta} + \sum_i \left(C_i\left(\Sigma_t^e + \Sigma_t^{\hat{x}} + 2\Sigma_t^{\hat{x}e}\right)C_i^T + \bar{C}_i L_t \Sigma_t^{\hat{\mathbf{x}}} L_t^T \bar{C}_i^T\right) + (A - K_tH)\Sigma_t^e A^T;\ \Sigma_1^e = \Sigma_1 \\
\Sigma_{t+1}^{\hat{x}} &= \left(A - BL_t\right)\Sigma_t^{\hat{x}}\left(A - BL_t\right)^T + K_tH\Sigma_t^e A^T + \left(A - BL_t\right)\Sigma_t^{\hat{\mathbf{x}}e}H^T K_t^T + K_tH\Sigma_t^{\hat{\mathbf{x}}e}\left(A - BL_t\right)^T + \Omega^{\eta};\ \Sigma_1^{\hat{x}} = \hat{\mathbf{x}}_1\hat{\mathbf{x}}_1^T \\
\Sigma_{t+1}^{\hat{\mathbf{x}}e} &= \left(A - BL_t\right)\Sigma_t^{\hat{\mathbf{x}}e}\left(A - K_tH\right)^T - \Omega^{\eta}
\end{aligned} \quad (0.28)$$

8. Optimal control of non-linear dynamics of reaching

The solution of optimal feedback controller was derived analytically for Linear Quadratic Gaussian (LQG) system with 'motor' and/or 'state' signal dependent noise, which guarantees global optimality. An important prediction of this model was the curved trajectories, i.e. the over-compensation. To what extent are these results affected if the system was a more realistic model of the arm? Here we will show that over-compensation is a fundamental property of the system.

The dynamic equation of two link arm is

$$\ddot{\theta} = M(\theta)^{-1}(\tau_u - \tau_e - a_2 \sin\theta_2 \begin{bmatrix} 2\dot{\theta}_1\dot{\theta}_2 + \dot{\theta}_2^2 \\ -\dot{\theta}_1^2 \end{bmatrix} - \begin{bmatrix} b_{11} & b_{12} \\ b_{21} & b_{22} \end{bmatrix}\begin{bmatrix} \dot{\theta}_1 \\ \dot{\theta}_2 \end{bmatrix})$$

where $[\theta_1, \theta_2]$ are shoulder and elbow joint angle, $M = \begin{bmatrix} a_1 + 2a_2\cos\theta_2 & a_3 + a_2\cos\theta_2 \\ a_3 + a_2\cos\theta_2 & a_3 \end{bmatrix}$,

$a_1 = I_1 + I_2 + m_2 l_1^2, a_2 = m_2 l_1 s_2, a_3 = I_2$, m_i are the link masses (1.4kg, 1kg), l_i are the link lengths (30cm, 33cm), s_i are the distances from the joint center to the center of the mass (11cm, 16cm), and I_i are the moment of inertia ($0.025kgm^2$, $0.045kgm^2$). b_* is a parameter of passive joint viscosity and we used $\begin{bmatrix} b_{11} & b_{12} \\ b_{21} & b_{22} \end{bmatrix} = \begin{bmatrix} 0.6 & 0.2 \\ 0.2 & 0.6 \end{bmatrix}$[Nms/rad]. τ_e is a torque due to the external force exerted at the

hand produced by the velocity dependent force field: $\mathbf{f}_D = D\mathbf{v}$, $D = \begin{bmatrix} 0 & 13 \\ -13 & 0 \end{bmatrix}$, where $\mathbf{f}_D, \mathbf{v}$ are the hand force and velocity of the hand. The virtual torque produced by the force field is $\tau_d = J(\theta)^T DJ(\theta)$, where $J(\theta) = \begin{bmatrix} -l_1 \sin(\theta_1) - l_2 \sin(\theta_1 + \theta_2) & -l_2 \sin(\theta_1 + \theta_2) \\ l_1 \cos(\theta_1) + l_2 \cos(\theta_1 + \theta_2) & l_2 \cos(\theta_1 + \theta_2) \end{bmatrix}$ is the Jacobian matrix of kinematics $d\mathbf{x} = Jd\theta$.

The cost was $w_u^J(\tau_1^2 + \tau_2^2)$ $(0 \le t < T)$, and $w_p^J(\theta_1 - \theta_1^*)^2 + w_p^J(\theta_2 - \theta_2^*)^2 + w_v^J(\dot{\theta}_1 + \dot{\theta}_2)$ $(T \le t < T + T_H)$, where θ^* is target position in joint coordinate system, reach duration T was 490 msec and simulation time $T + T_H$ was 500 msec. The weights of costs function were w_p^J =10, w_v^J =1 and $w_u^J = 0.1^8$ respectively. The task was reaching out to one of eight targets. The start position was at [0 ,0.45m] in the Cartesian coordinate system (where 0,0 is at the shoulder joint). The target was at 10 cm. The mathematics that we used to solve this problem is the same as that developed by (LI and Todorov, 2006), in which the nonlinear equations of forward dynamics are locally linearized and then solved as a linear optimal feedback control problem.

Figure S5 shows hand paths of optimal trajectory for Null and Force Field conditions (the field was a clockwise curl field). The trajectories were straight when no force was exerted at hand. As we expected, the trajectory curved so that trajectory could over-compensate the applied force, when the force field were exerted at hand. These predictions are very similar to the predictions of point-mass system regarding curvature of the over-compensation. However, the maximum of over-compensation of the simulation of two link arm was about 1cm which was slightly larger than that of observed data (<0.5cm). Thoroughman et al. (2007) had made a similar observation when performing these simulations under minimization of torque change or endpoint variance constraints. There are two possible reasons why amplitude of over-compensation was larger than measured data. First, it is very likely that subjects did not build perfect internal models. As we saw in the simulation of point mass system, the inaccuracy suppressed over-compensation. Independent measures suggest that during force field learning, adaptation is no better than 80% of maximum required force (Smith et al. 2006). Finally, it is possible that subjects had some extent of uncertainty for the force field environment due to noise inherently in the portion of state prediction in the brain. Increased uncertainty also tends to reduce the over-compensation.

References

Hamilton AF, Jones KE, Wolpert DM (2004) The scaling of motor noise with muscle strength and motor unit number in humans. Exp Brain Res 157:417-430.

Harris CM, Wlpert DM (1998) Signal-dependent noise determines motor planning. Nature 394:780-784.

Smith MA, Ghazizadeh A, Shadmehr R (2006) Interacting adaptive processes with different timescales underlie short-term motor learning. PLoS Biol 4:e179.

Thoroughman KA, Wang W, Tomov DN (2007) The influence of viscous loads on motor planning. J Neurophysiol.

Todorov E (2005) Stochastic optimal control and estimation methods adapted to the noise characteristics of the sensorimotor system. Neural Comput 17:1084-1108.

Todorov E, Jordan MI (2002) Optimal feedback control as a theory of motor coordination. Nat Neurosci 5:1226-1235.

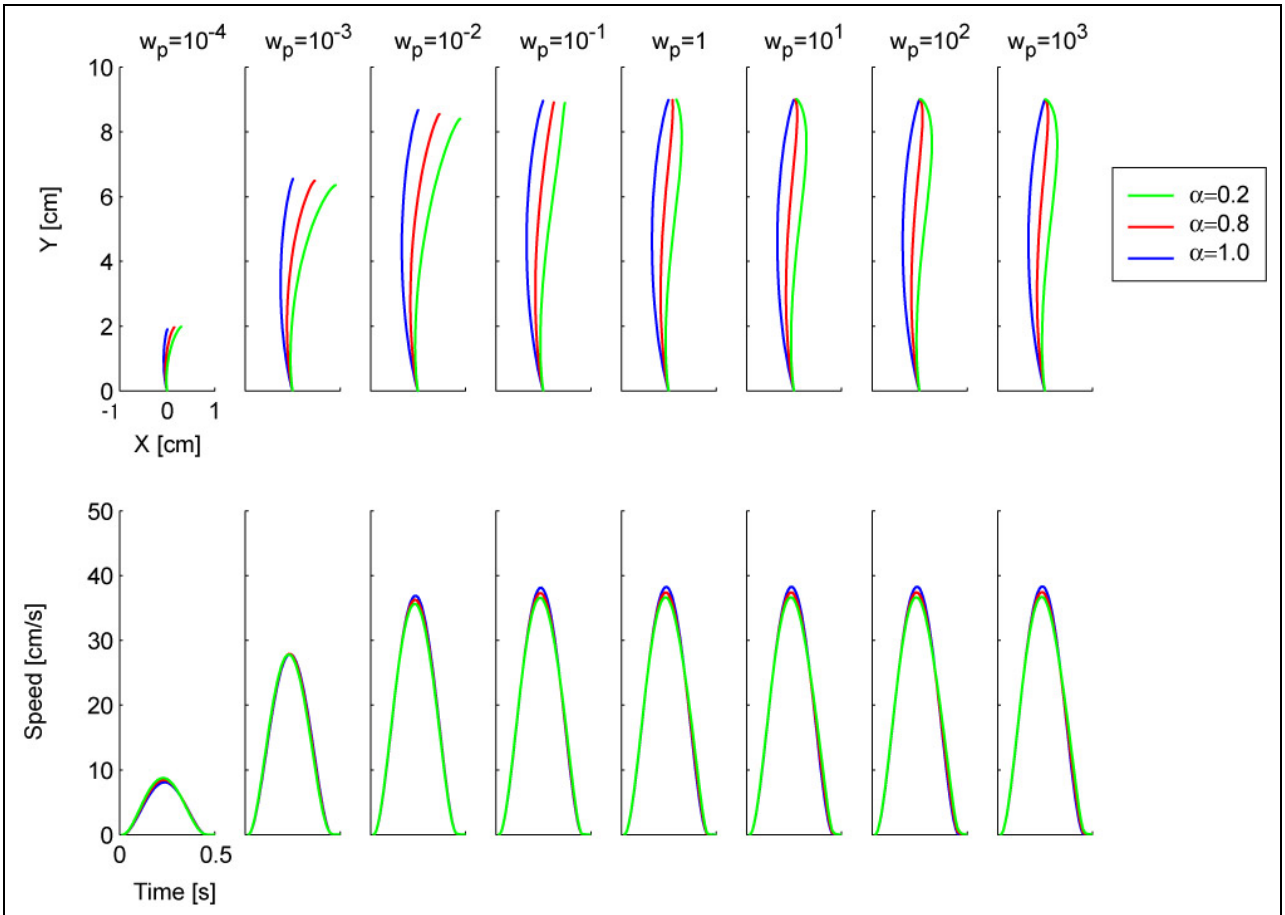

Figure S1. The effect of model bias and endpoint position costs on reach trajectory. Upper row: hand path. Bottom row: speed profile. Each column represents trajectory for a different value of weight of position cost w_p. Once endpoint costs are large enough so that the mass reaches the target, the effect of model bias is to reduce the over-compensation. There is no effect of model bias on reach speed.

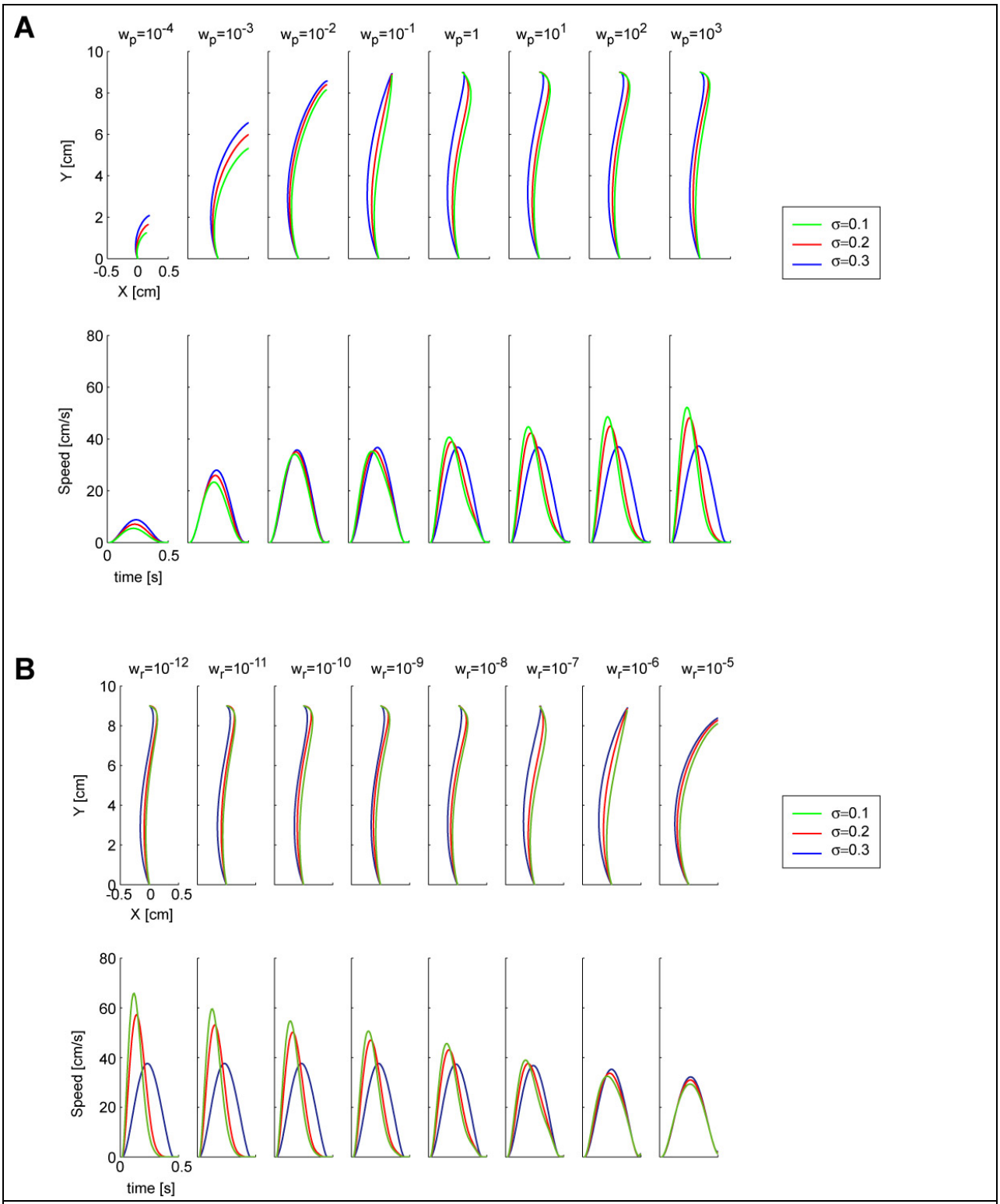

Figure S2. The effects of model uncertainty and costs on the reach to target task. **A**. Effects of endpoint costs w_p and model uncertainty. Upper row: hand path. Bottom row: speed profile. Model bias α is 0.8 for all simulations. B. Effects of motor cost w_r and model uncertainty.

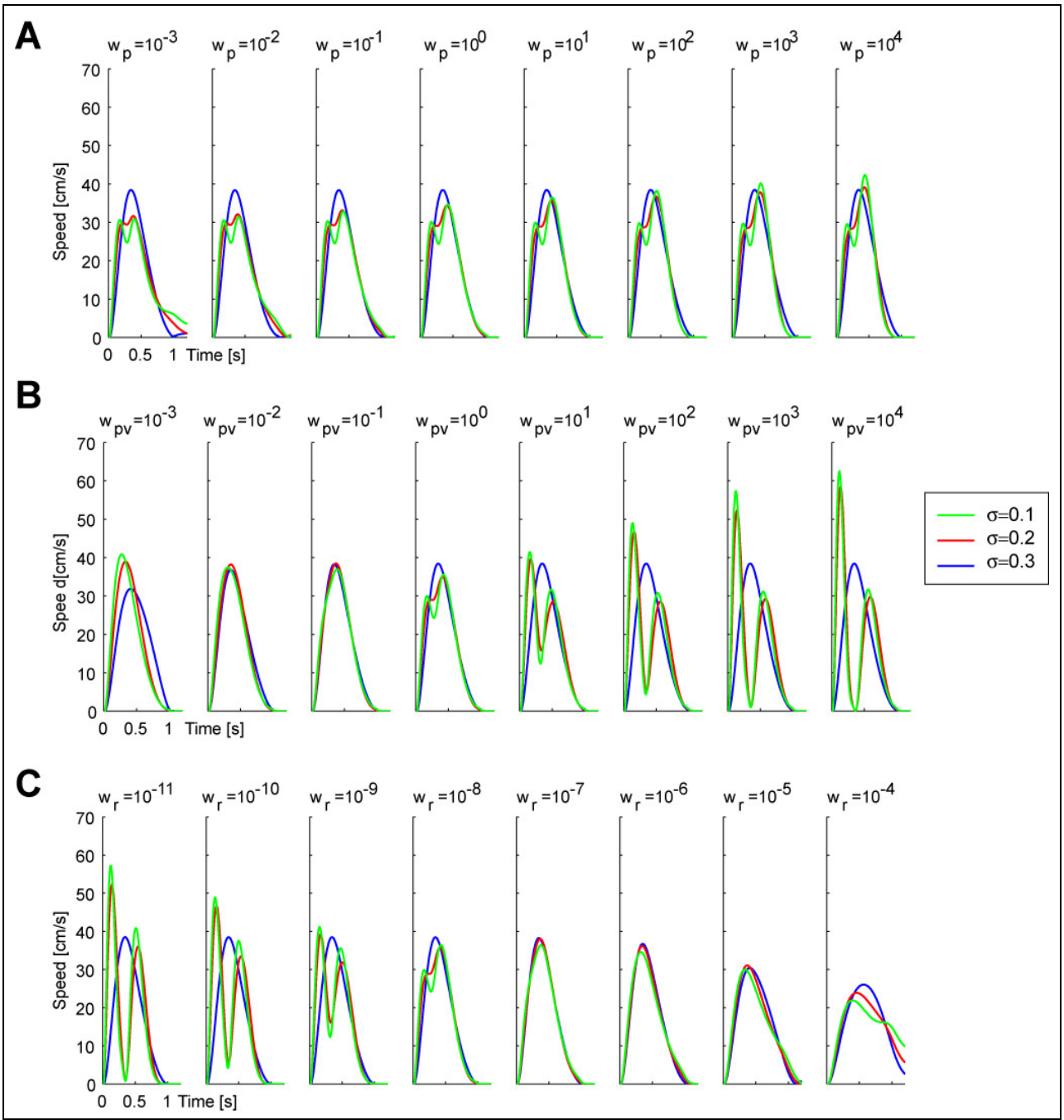

Figure S3. The effects of model uncertainty and costs on the via-point task. **A**. Speed profiles for different values of weight of position cost w_p. **B**. Speed profiles for different values of weight of via-point cost w_{pv}. **C**. Speed profiles for different values of weight of motor cost w_r.

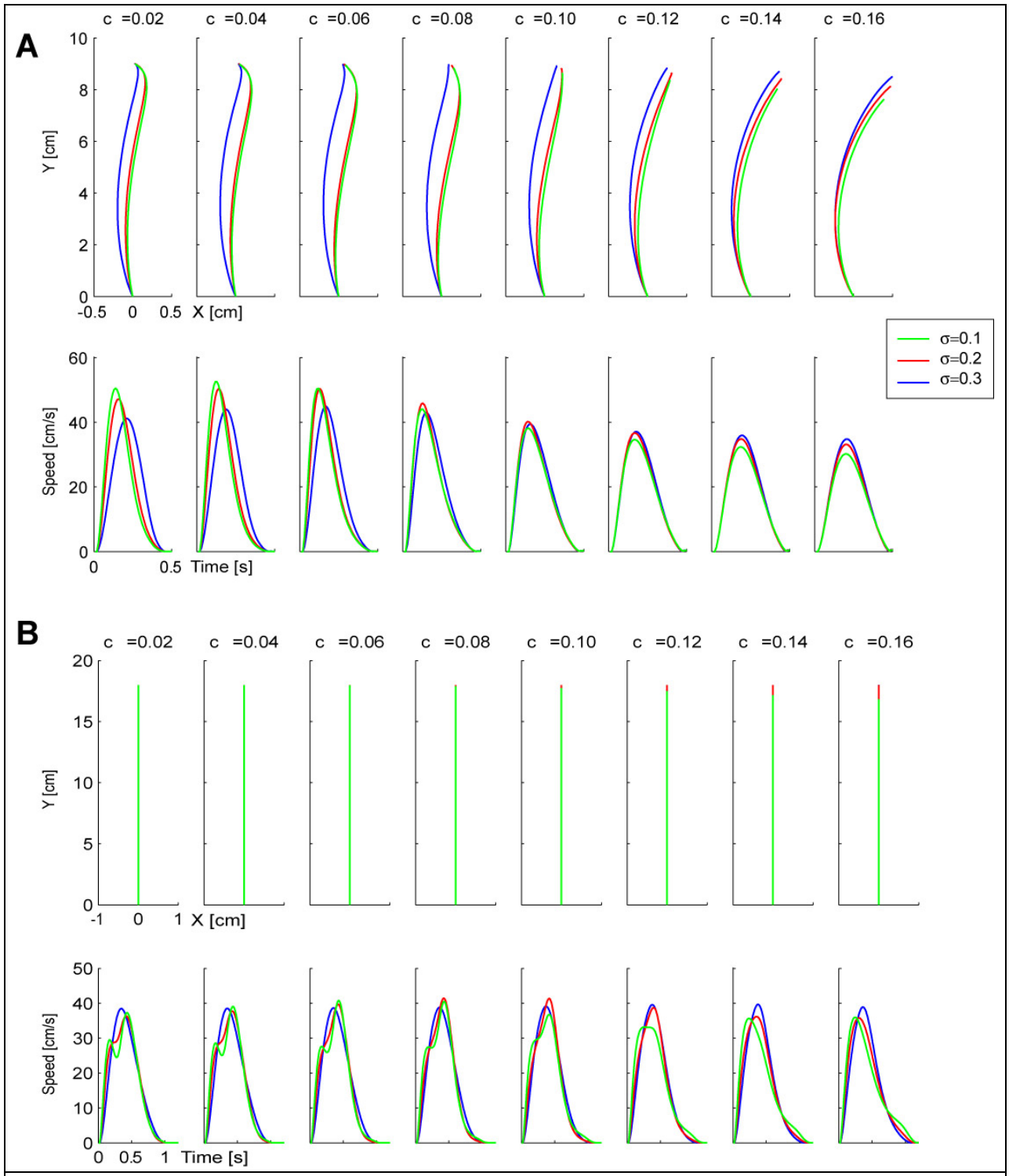

Figure S4. Effects of including signal dependent motor noise *c* for the reach to target and reach through the via-point simulations. Each line represents result of different amounts of model uncertainty. **A**. Reach to target simulations. **B**. Reach through a via-point simulations.

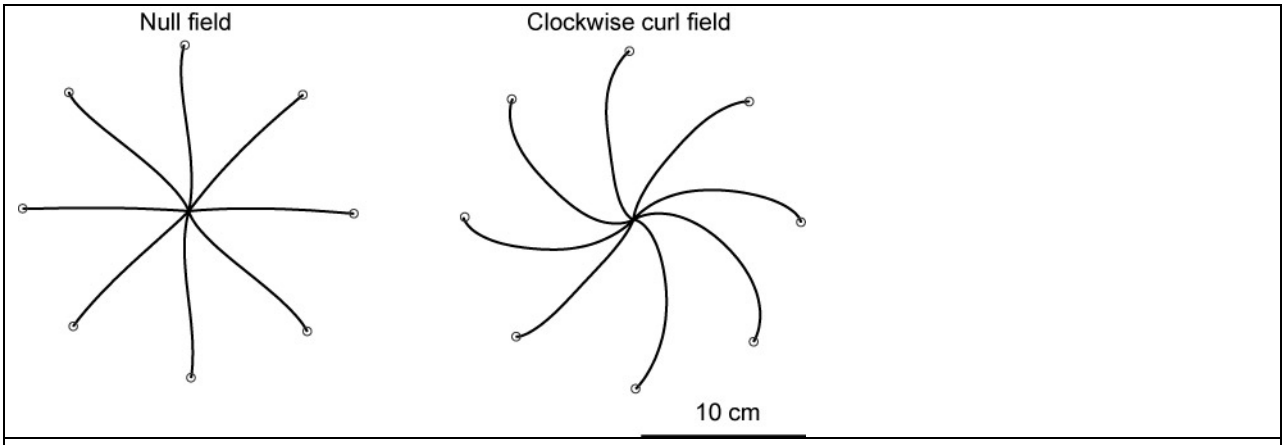

Figure S5. Hand paths of simulation of optimal control for a nonlinear model of arm dynamics. Left: Environment has zero forces (Null). Right: Environment has a clockwise curl force field. The small circles are target positions.